AAS 13-202

NONLINEAR FILTERING BASED ON TAYLOR DIFFERENTIAL ALGEBRA

Roberto Armellin,[*] Monica Valli,[†] Pierluigi Di Lizia,[‡] Michèle R. Lavagna,[§] and Renato Zanetti[¶]

The problem of nonlinear filtering represents a crucial issue in celestial mechanics. In this paper a high-order filter based on differential algebra is presented. The proposed filtering algorithm is based on nonlinear mapping of statistics and linear update scheme, in which only the pdf of the measurements is constrained to be Gaussian. No hypothesis on the state probability density function is made. The case of an Earth-orbiting spacecraft in a two-body problem frame is considered as an example to demonstrate the general feature and performance of the filter. A comparison with the extended and unscented Kalman filters is also included.

INTRODUCTION

Nonlinear filtering plays an important role in various space-related applications, especially in orbit determination and spacecraft navigation problems. A variety of missions in the near future demand accurate navigation systems able to perform accurate trajectory estimation in a very reduced lapse of time. Such missions include sample and return missions from small bodies, landing missions to the Moon, Mars and outer planets as well as interplanetary exploration.

At the present time the extended Kalman filter[1,2] (EKF) is the main algorithm used for trajectory estimation. To compute the estimation error covariance, the EKF relies on linearization of the equations of motion and the measurement equations via first-order Taylor series expansions centered at the current mean. In some cases this linearization assumption fails to provide an accurate representation of the estimate's uncertainty due to the nonlinearities involved. Low measurement frequency is also a factor in deteriorating the filter's consistency. In these cases, a different method that accounts for the system nonlinearity is preferred. An alternative approach is the unscented Kalman filter (UKF).[3,4] The UKF is also a linear estimator, but computes the covariance through a deterministic set of sigma points which can yield superior performance with respect to the EKF in producing a filter's covariance consistent with the actual estimation error. While the asymptotic complexity of the UKF algorithm is the same as for the EKF, the UKF is often slightly slower than the EKF. In 2007 Park and Scheeres[5,6] developed two nonlinear filters by implementing a semi-analytic orbit uncertainty propagation technique, that is by solving for the higher-order Taylor series terms that describe the localized nonlinear motion and by analytically mapping the initial uncertainties. These

[*]Postdoc Fellow, Aerospace Engineering Department, Politecnico di Milano, 20156 Milan, Italy
[†]Ph.D. Candidate, Aerospace Engineering Department, Politecnico di Milano, 20156 Milan, Italy
[‡]Postdoc Fellow, Aerospace Engineering Department, Politecnico di Milano, 20156 Milan, Italy
[§]Associate Professor, Aerospace Engineering Department, Politecnico di Milano, 20156 Milan, Italy
[¶]Senior Member of the Technical Staff, Vehicle Dynamics and Control, The Charles Stark Draper Laboratory, 17629 El Camino Real, Suite 470, Houston, Texas

higher-order filters are more accurate than the EKF, but the need to derive the so-called higher-order tensors makes them in many cases - especially for a sophisticated, high fidelity system model - difficult to use due to computational complexity. Up to now limited work has been done to automate and speed up the derivation of the state transition tensors.[7,8]

Differential algebraic (DA) techniques have been proposed in Valli et al.[9] as a valuable tool for efficient and accurate nonlinear uncertainty propagation. DA techniques supply the tools to compute the derivatives of functions within a computer environment.[10,11] More specifically, by substituting the classical implementation of real algebra with the implementation of a new algebra of Taylor polynomials, any function f of n variables is expanded into its Taylor polynomial up to an arbitrarily order m. This has a strong impact when the numerical integration of an ordinary differential equation (ODE) is performed by means of an arbitrary integration scheme. Any explicit integration scheme is based on algebraic operations, involving the evaluation of the ODE right hand side at several integration points. Therefore, starting from the DA representation of the initial conditions and carrying out all the evaluations in the DA framework, the flow of an ODE is obtained at each step as its Taylor expansion in the initial conditions. The accuracy of the Taylor expansion can be kept arbitrarily high by adjusting the expansion order. DA approach enabled the implementation of DA-based filters,[12] in which both the propagation of the mean trajectory and the measurement function evaluation are carried out in the DA framework. The obtained solution map not only provides the pointwise values for the propagated state and measurements, but also provides the higher-order partials of the solution flow and of the measurement equation. This eliminated the need to calculate the higher-order tensors at each time step by solving a complex system of augmented ODE. The main assumption of these methods is that the statistics of the state is described by a Gaussian probability density function (pdf).

In this work this assumption is removed. Whenever a new measurement becomes available, the observed data are mapped at a specific reference time as a Taylor polynomial of arbitrary order. This polynomial is used to update the estimate of the state variable and the related error statistics, without making any assumption on the estimated conditional pdf. The estimated statistics (i.e., the cumulants describing the pdf) can then be mapped forward or backward in time to represent the solution at any time of interest using the so called DA-based higher-order method (DAHO-k). The case of an Earth orbiting satellite with realistic initial orbit uncertainties and nonlinear measurements is presented to discuss the performances of the proposed filtering algorithm. Comparisons with EKF and UKF are used to support the conclusions.

The paper is organized as follows. First a brief introduction to differential algebra is given. Some hints on how to use it to expand the solution of parametric implicit equations and obtain high-order expansion of the flow are presented. Differential algebra is applied to obtain the nonlinear mapping of the statistics to demonstrate how the cumulants describing the pdf at a certain time can be mapped at any previous or later time. Then the proposed filtering technique is described. Finally, the effectiveness of the method is demonstrated through a numerical example.

NOTES ON DIFFERENTIAL ALGEBRA

DA techniques, exploited here to implement a high-order orbit determination algorithm, were devised to attempt solving analytical problems through an algebraic approach.[13] Historically, the treatment of functions in numerics has been based on the treatment of numbers, and the classical numerical algorithms are based on the mere evaluation of functions at specific points. DA techniques rely on the observation that it is possible to extract more information on a function rather than its

$$
\begin{tikzcd}
a, b \in R \arrow[r, "\mathcal{T}"] \arrow[d, "\times"'] & \overline{a}, \overline{b} \in FP \arrow[d, "\otimes"] \\
a \times b \arrow[r, "\mathcal{T}"'] & \overline{a} \otimes \overline{b}
\end{tikzcd}
\qquad
\begin{tikzcd}
f, g \arrow[r, "\mathcal{T}"] \arrow[d, "\times"'] & F, G \arrow[d, "\otimes"] \\
f \times g \arrow[r, "\mathcal{T}"'] & F \otimes G
\end{tikzcd}
$$

Figure 1: Analogy between the floating point representation of real numbers in a computer environment (left figure) and the introduction of the algebra of Taylor polynomials in the differential algebraic framework (right figure).

mere values. The basic idea is to bring the treatment of functions and the operations on them to computer environment in a similar manner as the treatment of real numbers. Referring to Figure 1, consider two real numbers a and b. Their transformation into the floating point representation, $\overline{a}$ and $\overline{b}$ respectively, is performed to operate on them in a computer environment. Then, given any operation $*$ in the set of real numbers, an adjoint operation $\circledast$ is defined in the set of floating point (FP) numbers so that the diagram in Figure 1 commutes. (The diagram commutes approximately in practice due to truncation errors.) Consequently, transforming the real numbers a and b into their FP representation and operating on them in the set of FP numbers returns the same result as carrying out the operation in the set of real numbers and then transforming the achieved result in its FP representation. In a similar way, let us suppose two k differentiable functions f and g in n variables are given. In the framework of differential algebra, the computer operates on them using their k-th order Taylor expansions, F and G respectively. Therefore, the transformation of real numbers in their FP representation is now substituted by the extraction of the k-th order Taylor expansions of f and g. For each operation in the space of k differentiable functions, an adjoint operation in the space of Taylor polynomials is defined so that the corresponding diagram commutes; i.e., extracting the Taylor expansions of f and g and operating on them in the space of Taylor polynomials (labeled as ${}_kD_n$) returns the same result as operating on f and g in the original space and then extracting the Taylor expansion of the resulting function. The straightforward implementation of differential algebra in a computer allows computation of the Taylor coefficients of a function up to a specified order k, along with the function evaluation, with a fixed amount of effort. The Taylor coefficients of order n for sums and products of functions, as well as scalar products with reals, can be computed from those of summands and factors; therefore, the set of equivalence classes of functions can be endowed with well-defined operations, leading to the so-called truncated power series algebra.[14,15] Similarly to the algorithms for floating point arithmetic, the algorithms for functions followed, including methods to perform composition of functions, to invert them, to solve nonlinear systems explicitly, and to treat common elementary functions.[13,16] In addition to these algebraic operations, the DA framework is endowed with differentiation and integration operators, therefore finalizing the definition of the DA structure. The DA sketched in this section was implemented by M. Berz and K. Makino in the software COSY INFINITY.[17]

Expansion of the solution of parametric implicit equations

Well-established numerical techniques (e.g., Newton's method) exist, which can effectively identify the solution of a classical implicit equation

$$f(x) = 0. \tag{1}$$

Suppose an explicit dependence on a vector of parameters $\boldsymbol{p}$ can be highlighted in the previous function f, which leads to the parametric implicit equation

$$f(x, \boldsymbol{p}) = 0. \tag{2}$$

Suppose the previous equation is to be solved, whose solution is represented by the function $x(\boldsymbol{p})$ returning the value of x solving (2) for any value of $\boldsymbol{p}$. Thus, the dependence of the solution of the implicit equation on $\boldsymbol{p}$ is of interest. DA techniques can effectively handle the previous problem by identifying the function $x(\boldsymbol{p})$ in terms of its Taylor expansion with respect to $\boldsymbol{p}$. The DA-based algorithm is presented in the following for the solution of the scalar parametric implicit Eq. (2); the generalization to a system of parametric implicit equations is straightforward.

The solution of (2) is sought, where sufficient regularity is assumed to characterize the function f; i.e., $f \in \mathcal{C}^k$. This means that $x(\boldsymbol{p})$ satisfying

$$f(x(\boldsymbol{p}), \boldsymbol{p}) = 0 \tag{3}$$

is to be identified. The first step is to consider a reference value of $\boldsymbol{p}$ and to compute the solution x by means of a classical numerical method; e.g., Newton's method. The variable x and the parameter $\boldsymbol{p}$ are then initialized as k-th order DA variables, i.e.,

$$\begin{aligned} [x] &= x + \delta x \\ [\boldsymbol{p}] &= \boldsymbol{p} + \delta \boldsymbol{p}. \end{aligned} \tag{4}$$

A DA-based evaluation of the function f in (2) delivers the k-th order expansion of f with respect to x and $\boldsymbol{p}$:

$$\delta f = \mathcal{M}_f(\delta x, \delta \boldsymbol{p}), \tag{5}$$

where $\mathcal{M}_f$ denotes the Taylor map for f. Note that the Map (5) is origin-preserving as x is the solution of the implicit equation for the nominal value of $\boldsymbol{p}$; thus, δf represents the deviation of f from its reference value. Map (5) is then augmented by introducing the map corresponding to the identity function on $\boldsymbol{p}$ (i.e., $\delta \boldsymbol{p} = \mathcal{I}_{\boldsymbol{p}}(\delta \boldsymbol{p})$) ending up with

$$\begin{bmatrix} \delta f \\ \delta \boldsymbol{p} \end{bmatrix} = \begin{bmatrix} \mathcal{M}_f \\ \mathcal{I}_{\boldsymbol{p}} \end{bmatrix} \begin{bmatrix} \delta x \\ \delta \boldsymbol{p} \end{bmatrix}. \tag{6}$$

The k-th order Map (6) is inverted using COSY-Infinity built-in tools (based on fixed point iterations), obtaining

$$\begin{bmatrix} \delta x \\ \delta p \end{bmatrix} = \begin{bmatrix} \mathcal{M}_f \\ \mathcal{I}_{\boldsymbol{p}} \end{bmatrix}^{-1} \begin{bmatrix} \delta f \\ \delta \boldsymbol{p} \end{bmatrix}. \tag{7}$$

As the goal is to compute the k-th order Taylor expansion of the solution manifold $x(\boldsymbol{p})$ of (2), the map (7) is evaluated for $\delta f = 0$

$$\begin{bmatrix} \delta x \\ \delta \boldsymbol{p} \end{bmatrix} = \begin{bmatrix} \mathcal{M}_f \\ \mathcal{I}_{\boldsymbol{p}} \end{bmatrix}^{-1} \begin{bmatrix} 0 \\ \delta \boldsymbol{p} \end{bmatrix}. \tag{8}$$

The first row of Map (8)

$$\delta x = \mathcal{M}_x(\delta \boldsymbol{p}), \tag{9}$$

expresses how a variation of the parameter $\delta \boldsymbol{p}$ affects the solution of the implicit equation as a k-th order Taylor polynomial. In particular, by plugging Map (8) in first of (4) we obtain

$$[x] = x + \mathcal{M}_x(\delta \boldsymbol{p}), \tag{10}$$

which is the k-th order Taylor expansion of the solution of the implicit equation. For every value of $\delta \boldsymbol{p}$, the approximate solution of $f(x, \boldsymbol{p}) = 0$ can be easily computed by evaluating the Taylor polynomial (10). Apparently, the solution obtained by means of Map (10) is a Taylor approximation of the exact solution of Eq. (2). The accuracy of the approximation depends on both the order of the Taylor expansion and the displacement $\delta \boldsymbol{p}$ from the reference value of the parameter.

Within this work, the algorithm just introduced is utilized for expanding the solution of Kepler's equation that appear in the two-body problem and to implement the high-order filter algorithm. In this section the classical form of Kepler's equation is considered

$$\sqrt{\frac{\mu}{a^3}}\, t = E - e \sin E, \tag{11}$$

in which μ is the gravitational parameter of the attractor, a the semi-major axis, t the time since pericenter passage, e the eccentricity, and E the unknown eccentric anomaly. Let us work in adimensional variables, such that $\mu = 1$, $a = 1$, and thus the orbital period is $T = 2\pi$. For the sake of illustrative purposes, we expand the solution of Kepler's equation in Taylor series with respect to $\boldsymbol{p} = (a, e)$ around the nominal condition $\boldsymbol{p} = (1, 0.5)$. We also fix $t = \pi$, so that $E = \pi$ is the nominal solution. The first step to approximate the solution manifold $E = E(a, e)$ in Taylor series is to initialize E, a, and e as DA variables

$$\begin{array}{rcl} [E] & = & \pi + \delta E \\ [a] & = & 1 + \delta a \\ [e] & = & 0.5 + \delta e. \end{array} \tag{12}$$

The algorithm described by Eq.s (5)–(9) is then applied to the implicit equation

$$f\left(E(a, e), a, e\right) = \sqrt{\frac{\mu}{a^3}}\, t - E + e \sin E = 0. \tag{13}$$

The result is $[E] = \pi + \mathcal{M}_E(\delta a, \delta e)$, which is a Taylor polynomial of arbitrary order k.

Figure 2(a) shows some contour lines of $[E]$ for $a \in [0.9, 1.1]$ and $e \in [0.4, 0.6]$ for a sixth order computation. The Taylor expansion is capable of accurately representing the solution $E = \pi$ for $a = 1$. In Figure 2(b) the accuracy of the expansion is studied in logarithmic scale. Taylor polynomial evaluations are compared with the solutions of Kepler's equation obtained by applying point-wise Newton's iterations on a fine grid in the a-e plane. It is apparent that the expansion error decreases significantly close to the reference point and, in addition, the polynomial approximation is exact for the entire line $a = 1$. The computational time for the computation of the sixth order expansion is 0.45×10^{-3} s on an Intel Core 2 Duo @2.4GHz, running on a Mac OS X 10.6.8. (All the computations presented in the manuscript are performed on this machine.) As a last comment, note that the solution of the two-body problem involves a different form of Kepler's equation. Furthermore, its solution is expanded in Taylor series with respect to uncertainties in the entire initial state (i.e., we have Taylor polynomials of six variables).

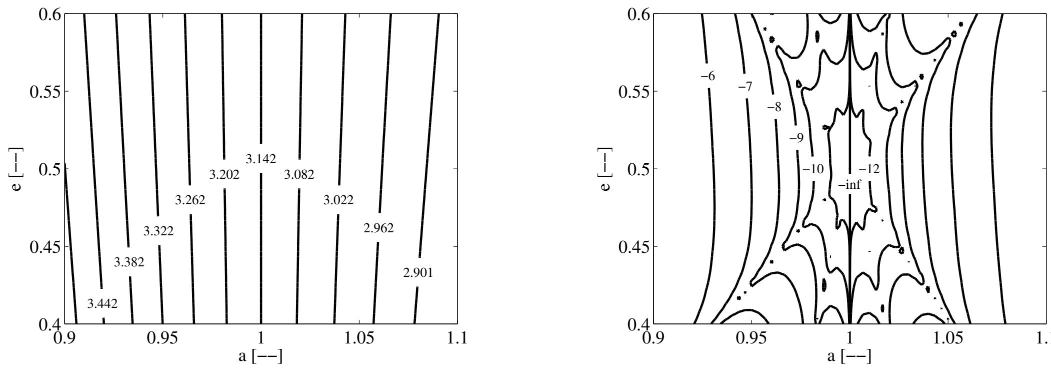

(a) Contour lines of E obtained by evaluating the Taylor map. The solution is $E = \pi$ for $a = 1$.

(b) Contour lines of the logarithm of the expansion error. The expansion error is zero for $a = 1$.

Figure 2: Kepler's equation: sixth order Taylor expansion of $E(a, e)$.

High-order expansion of the flow

The differential algebra allows the derivatives of any function f of n variables to be computed up to an arbitrary order k, along with the function evaluation. This has an important consequence when the numerical integration of an ODE is performed by means of an arbitrary integration scheme. Any integration scheme is based on algebraic operations, involving the evaluation of the ODE right hand side at several integration points. Therefore, carrying out all the evaluations in the DA framework allows differential algebra to compute the arbitrary order expansion of the flow of a general ODE with respect to the initial condition.

Without loss of generality, consider the scalar initial value problem

$$\begin{cases} \dot{x} = f(x, t) \\ x(t_0) = x_0 \end{cases} \tag{14}$$

and the associated phase flow $\varphi(t; x_0)$. We now want to show that, starting from the DA representation of the initial condition x_0, differential algebra allows us to propagate the Taylor expansion of the flow in x_0 forward in time, up to the final time t_f.

Replace the point initial condition x_0 by the DA representative of its identity function up to order k, which is a $(k + 1)$-tuple of Taylor coefficients. (Note that x_0 is the flow evaluated at the initial time; i.e, $x_0 = \varphi(t_0; x_0)$.) As for the identity function only the first two coefficients, corresponding to the constant part and the first derivative respectively, are non zeros, we can write $[x_0]$ as $x_0 + \delta x_0$, in which x_0 is the reference point for the expansion. If all the operations of the numerical integration scheme are carried out in the framework of differential algebra, the phase flow $\varphi(t; x_0)$ is approximated, at each fixed time step t_i, as a Taylor expansion in x_0.

For the sake of clarity, consider the forward Euler's scheme

$$x_i = x_{i-1} + f(x_{i-1})\Delta t \tag{15}$$

and substitute the initial value with the DA identity $[x_0] = x_0 + \delta x_0$. At the first time step we have

$$[x_1] = [x_0] + f([x_0]) \cdot \Delta t. \tag{16}$$

If the function f is evaluated in the DA framework, the output of the first step, $[x_1]$, is the k-th order Taylor expansion of the flow $\varphi(t; x_0)$ in x_0 for $t = t_1$. Note that, as a result of the DA evaluation of $f([x_0])$, the $(k+1)$-tuple $[x_1]$ may include several non zeros coefficients corresponding to high-order terms in δx_0. The previous procedure can be inferred through the subsequent steps. The result of the final step is the k-th order Taylor expansion of $\varphi(t; x_0)$ in x_0 at the final time t_f. Thus, the flow of a dynamical system can be approximated, at each time step t_i, as a k-th order Taylor expansion in x_0 in a fixed amount of effort.

The conversion of standard integration schemes to their DA counterparts is straightforward both for explicit and implicit solvers. This is essentially based on the substitution of the operations between real numbers with those on DA numbers. In addition, whenever the integration scheme involves iterations (e.g. iterations required in implicit and predictor-corrector methods), step size control, and order selection, a measure of the accuracy of the Taylor expansion of the flow needs to be included.

The main advantage of the DA-based approach is that there is no need to write and integrate variational equations in order to obtain high-order expansions of the flow. This result is basically obtained by the substitution of operations between real numbers with those on DA numbers, and therefore the method is ODE independent. Furthermore, the efficient implementation of the differential algebra in COSY-Infinity allows us to obtain high-order expansions with limited computational time. Integration schemes based on DA pave the way to the nonlinear mapping of uncertainties necessary for the implementation of the proposed orbit determination algorithm for an arbitrarily complex dynamical system. A first example is presented hereafter about the propagation of uncertainties on initial conditions.

UNCERTAINTY PROPAGATION

Before focusing on nonlinear filtering, let us consider the problem of uncertainty propagation through nonlinear dynamics. As we will see later on, the nonlinear filtering technique presented in this paper uses the measurements to update the estimated pdf at a specified time. This pdf must then be propagated forward/backward in time in order to describe the solution at any time of interest. In this section we will discuss how this propagation can be done.

So, let us consider the general case of an arbitrary nonlinear transformation. Depending on the study case, the considered nonlinear transformation can have different meanings; i.e., a coordinate transformation, the nonlinear dynamical evolution of a physical system, and so on. However, independently of these single cases, the techniques presented hereafter can be used and remain valid whenever the problem of propagating the statistics of a system through an arbitrary nonlinear function must be solved. Moreover, in many cases of practical interest - and in particular in celestial mechanics and orbit estimation - the Gaussian assumption can not provide a sufficiently accurate statistical approximation of the transformed pdf. Hence, the problem of uncertainty propagation through nonlinear transformations becomes one of computing not only the estimate of the transformed mean and covariance, but also of the higher order cumulants.

Nonlinear mapping of the estimate statistics

Consider random variable $\boldsymbol{x} \in \Re^n$ with probability density function $p(\boldsymbol{x})$ and a second random variable $\boldsymbol{y}$ related to $\boldsymbol{x}$ through the nonlinear transformation

$$\boldsymbol{y} = \boldsymbol{f}(\boldsymbol{x}). \tag{17}$$

The problem is to calculate a consistent estimate of the main cumulants of the transformed probability density function $p(\boldsymbol{y})$. As said before, since $\boldsymbol{f}$ is a generic nonlinear function this formulation includes a wide range of problems involving uncertainty propagation (uncertainty propagation through nonlinear dynamics, uncertainty propagation through nonlinear coordinate transformations, etc.).

Define independent variable $\boldsymbol{x}$ as a DA variable

$$[\boldsymbol{x}] = \bar{\boldsymbol{x}} + \delta\boldsymbol{x}, \tag{18}$$

where $\bar{\boldsymbol{x}}$ is the initial mean, and implement the nonlinear transformation in DA framework up to order k. The result is the Taylor expansion of the final solution with respect to deviations $\boldsymbol{\delta}x$ of the independent variable

$$[\boldsymbol{y}] = \boldsymbol{f}([\boldsymbol{x}]) = \bar{\boldsymbol{y}} + \mathcal{M}_{\boldsymbol{y}}(\delta\boldsymbol{x}) = \sum_{p_1+\cdots+p_n \leq k} \boldsymbol{c}_{p_1\ldots p_n} \cdot \delta x_1^{p_1} \cdots \delta x_n^{p_n}, \tag{19}$$

where $\bar{\boldsymbol{y}}$ is the zeroth order term of the expansion map, and $\boldsymbol{c}_{p_1\ldots p_n}$ are the Taylor coefficients of the resulting Taylor polynomial

$$\boldsymbol{c}_{p_1\ldots p_n} = \frac{1}{p_1! \cdots p_n!} \cdot \frac{\partial^{p_1+\cdots+p_n}\boldsymbol{f}}{\partial x_1^{p_1} \cdots \partial x_n^{p_n}}. \tag{20}$$

If an ODE system in the form (14) is considered, Eq. (19) remains unchanged and $\boldsymbol{c}_{p_1\ldots p_n}$ become the terms that relate deviations in the initial conditions to the state at some future time. Park and Scheeres[18] called this operator of higher-order partials of the state the state transition tensor (STT). Note that the case $k = 1$ corresponds to the ordinary first-order statistics propagation (i.e., the approximation corresponding to a linearized model), where $\boldsymbol{c}_{p_1\ldots p_n}$ are elements of the well-known state transition matrix. The evaluation of (19) for a selected value of $\delta\boldsymbol{x}$ supplies the k-th order Taylor approximation of the solution $\boldsymbol{y}$ corresponding to the displaced independent variable. Of course, the accuracy of the expansion map is function of the expansion order and can be controlled by tuning it. As already said, DA techniques allow the computation of derivatives up to order k of functions in n variables (i.e., the coefficients $\boldsymbol{c}_{p_1\ldots p_n}$ of the Taylor series) and the approximation of the original function in the space of Taylor polynomials. So, contrary to other methods, such as the UT, that are founded on the idea that it is easier to approximate a pdf than it is to approximate an arbitrary nonlinear function, the starting point and foundation of our approach is the straightforward approximation of the function itself.

The Taylor series in the form (19) can be used to efficiently compute the propagated statistics. The method consists in analytically describing the statistics of the solution by computing the l-th moment of the transformed pdf using a proper form of the l-th power of the solution Map (19). This numerical procedure will be referred to as DAHO-k method, where DAHO stands for "DA-based higher-order" and k indicates the expansion order.

DAHO-k method

For a generic scalar random variable z with pdf $g(z)$ the first four moments can be written as

$$\begin{cases} \mu = E\{z\} \\ P = E\{(z-\mu)^2\} \\ \gamma = \dfrac{E\{(z-\mu)^3\}}{\sigma^3} \\ \kappa = \dfrac{E\{(z-\mu)^4\}}{\sigma^4} - 3, \end{cases} \tag{21}$$

where μ is the mean value, P is the covariance, γ and κ are the skewness and the kurtosis, respectively,[19] and the expectation value of z is defined as

$$E\{z\} = \int_{-\infty}^{+\infty} z g(z) dz. \tag{22}$$

So, the moments of the transformed pdf for problem (17) can be computed by applying the multivariate form of Eq. (21) to the Taylor expansion (19). The result for the first two moments becomes

$$\begin{cases} \boldsymbol{\mu}_i = E\{[\boldsymbol{y}_i]\} = \displaystyle\sum_{p_1+\cdots+p_n\leq k} \boldsymbol{c}_{i,p_1\ldots p_n} E\{\delta x_1^{p_1}\cdots\delta x_n^{p_n}\} \\ \boldsymbol{P}_{ij} = E\{([\boldsymbol{y}_i]-\boldsymbol{\mu}_i)([\boldsymbol{y}_j]-\boldsymbol{\mu}_j)\} = \displaystyle\sum_{\substack{p_1+\cdots+p_n\leq k,\\ q_1+\cdots+q_n\leq k}} \boldsymbol{c}_{i,p_1\ldots p_n}\boldsymbol{c}_{j,q_1\ldots q_n} E\{\delta x_1^{p_1+q_1}\cdots\delta x_n^{p_n+q_n}\}, \end{cases} \tag{23}$$

where $\boldsymbol{c}_{i,p_1\ldots p_n}$ are the Taylor coefficients of the Taylor polynomial describing the i-th component of $[\boldsymbol{y}]$. Note that in the covariance matrix formula the coefficients $\boldsymbol{c}_{i,p_1\ldots p_n}$ and $\boldsymbol{c}_{j,q_1\ldots q_n}$ already include the subtraction of the mean terms. The coefficients of the higher order moments are computed by implementing the required operations (e.g. $([\boldsymbol{y}_i]-\boldsymbol{\mu}_i)([\boldsymbol{y}_j]-\boldsymbol{\mu}_j)$ for the second order moment) on Taylor polynomials in the DA framework. The expectation values on the right side of Eq. (23) are function of $p(\boldsymbol{x})$. It follows that if the initial distribution is known, all of the moments of the transformed pdf $p(\boldsymbol{y})$ can be calculated. The number of monomials for which it is necessary to compute the expectation increases with the order of the Taylor expansion and, of course, with the order of the moment we want to compute. Note that, at this time, no hypothesis on the initial pdf has been made. Thus, the method can be applied independently of the considered variable distribution.

For the purpose of illustration and without loss of generality, we now restrict to the case where $\boldsymbol{x}$ is a Gaussian random variable (GRV), $\boldsymbol{x} \sim \mathcal{N}(\boldsymbol{\mu}, \boldsymbol{P})$, in which $\boldsymbol{\mu}$ is the mean vector and $\boldsymbol{P}$ the covariance matrix.

An important property of Gaussian distributions is that the statistics of a GRV can be completely described by the first two moments. In case of zero mean, the expression for computing higher-order moments in terms of the covariance matrix is due to Isserlis.[20] In physics literature, Isserlis's formula is known as the Wick's formula.

Let s_1 to s_n be nonnegative integers, and $s = s_1 + s_2 + \cdots + s_n$. Then the Wick's formula suggests that

$$E\{x_1^{s_1}x_2^{s_2}\ldots x_n^{s_n}\} = \begin{cases} 0, & \text{if } s \text{ is odd} \\ Haf(\boldsymbol{P}), & \text{if } s \text{ is even} \end{cases} \tag{24}$$

where $Haf(\boldsymbol{P})$ is the hafnian of $P = (\sigma_{ij})$, which is defined as

$$Haf(\boldsymbol{P}) = \sum_{p \in \prod_s} \prod_{i=1}^{\frac{s}{2}} \sigma_{p_{2i-1}, p_{2i}}, \tag{25}$$

and $\prod_s$ is the set of all permutations p of $\{1, 2, \ldots, s\}$ satisfying the property $p_1 < p_3 < p_5 < \ldots < p_{s-1}$ and $p_1 < p_2,\ p_3 < p_4, \ldots, p_{s-1} < p_s$.[21]

We observe that the expectation value terms of Eq. (23) can be computed using Eq. (24), and the resulting moments can be used to describe the transformed pdf.

The DAHO-k method can be placed in the framework of higher order Taylor series methods for uncertainty propagation. However, the classical methods that utilize the state transition tensor approach[18,22] need to calculate the higher-order partial derivatives by writing and numerically integrating the high-order variational equations, which makes these methods complex and computationally expensive for nontrivial problems. The differential algebra approach does not require to write any additional set of equations, as the arbitrary high-order expansion of the flow is a straightforward result of the implemented algebra.

Numerical example

The framework described thus far has been applied to a typical problem in celestial mechanics. More in detail, the problem of uncertainty propagation through the nonlinear dynamics of an artificial Earth-orbiting satellite is addressed. The second-order differential equation governing the motion is

$$\frac{d\ddot{\boldsymbol{r}}}{dt} = -\frac{\mu}{r^3}\boldsymbol{r}, \tag{26}$$

where $\boldsymbol{r}$ is the position vector of the spacecraft and μ is the Earth gravitational parameter. The initial position and velocity assumed for the analysis, defined as DA variables, are

$$\boldsymbol{x}_0 = \begin{pmatrix} \boldsymbol{r}_0 \\ \boldsymbol{v}_0 \end{pmatrix} = \begin{pmatrix} -0.68787 + \delta x \\ -0.39713 + \delta y \\ +0.28448 + \delta z \\ -0.51331 + \delta v_x \\ +0.98266 + \delta v_y \\ +0.37611 + \delta v_z \end{pmatrix}, \tag{27}$$

and the initial covariance matrix is a diagonal matrix with variance 10^{-5} for the position vector components and 10^{-7} for the velocity vector components. The length units are scaled by the orbit semi-major axis (a=8788 km) and the time by $\sqrt{\frac{a^3}{\mu}}$. (For the sake of completeness, other relevant orbital parameters are $e = 0.1712$ and $i = 153.25$ deg).

The simulation results related to the first two components of the state vector for different propagation times are presented in Table 1. (Note that the orbital propagation can be performed either by the expansion of the solution of Kepler's equation as described in section *Expansion of the solution of parametric implicit equations* or by DA numerical integration as explained in section *High-order expansion of the flow*). In the last column of the table, the results of a DA-based Monte Carlo simulation of eighth order (labeled as DAMC$_8$ and here used as a reference solution to assess the performance of the DAHO-k method) are shown. Figures 3 and 4 show the propagated samples

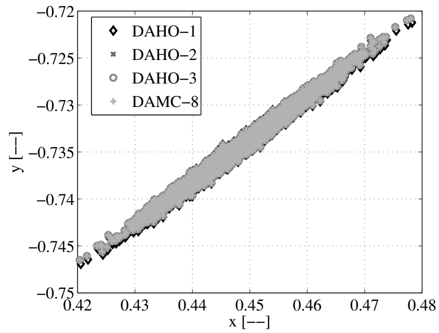

(a) Samples distribution after 0.8 orbit

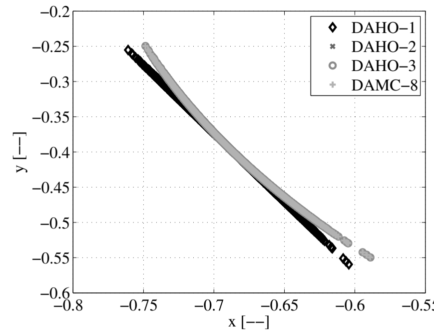

(b) Samples distribution after 5 orbits

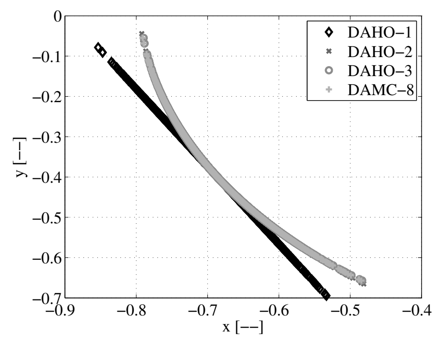

(c) Samples distribution after 10 orbits

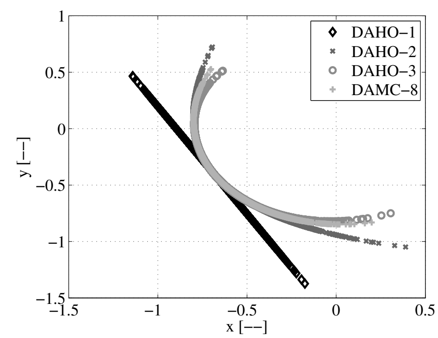

(d) Samples distribution after 30 orbits

Figure 3: Propagated samples distribution projection on the x-y plane for the 2-body dynamics test case.

distribution and the related uncertainty ellipses for different propagation times. From these results it is apparent that the system's nonlinearity makes the linearized solution quite inaccurate already after few orbits. On the other hand, the DAHO-k method provides a solution that increases its accuracy in accordance with the method's order k. From a more general point of view, the obtained results show how the DAHO-k method can be successfully applied to propagate an arbitrary pdf (i.e., the pdf's main cumulants) from one time to another, becoming a fundamental tool to process the solution of the proposed filtering algorithm.

THE DA-BASED MAP INVERSION NONLINEAR FILTER (DA-BASED MIF)

In the previous section we showed how a pdf can be mapped forward in time through a nonlinear dynamical system. Now we introduce a high-order filtering technique based on nonlinear mapping of statistics and linear update scheme, in which only the pdf of the measurements is constrained to be Gaussian.

Consider a time span $[t_0, t_f]$ and let $\boldsymbol{x}_k$ be the state variable at some time $t_k \in [t_0, t_f]$. Consider also a set of N measurements $\boldsymbol{y}_i$ given at time t_i with $i = 1, \ldots, N$. Given the current estimate of the state $\boldsymbol{m}_k^-$ and the related error statistics, we can always define the estimated state as a DA variable and compute in the DA framework the predicted measurement, obtaining the Taylor expansion Map $\boldsymbol{y}_i = \boldsymbol{f}(\boldsymbol{x}_k)$. Function $\boldsymbol{f}$ represents a nonlinear map that includes the flow of the dynamics

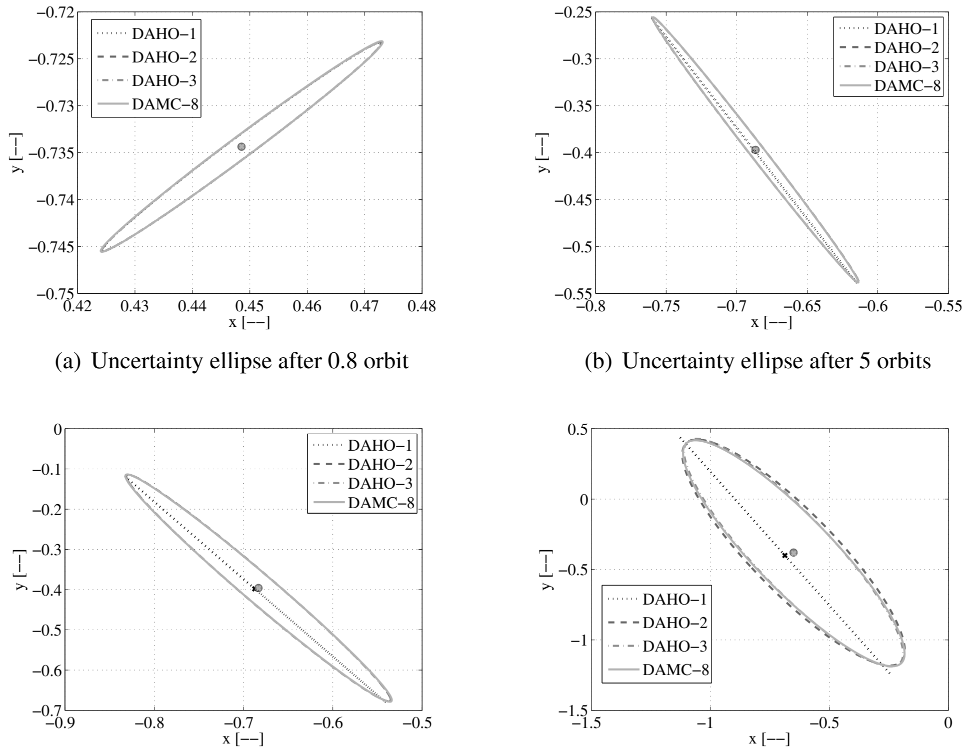

(a) Uncertainty ellipse after 0.8 orbit

(b) Uncertainty ellipse after 5 orbits

(c) Uncertainty ellipse after 10 orbits

(d) Uncertainty ellipse after 30 orbits

Figure 4: Propagated mean and 3-σ uncertainty ellipse projection on the x-y plane for the 2-body dynamics test case.

	DAHO-1	DAHO-2	DAHO-3		DAMC-8
Propagation time = 0.8 orbits					
$\Delta\mu_x$ [%]	8.005×10^{-3}	5.890×10^{-3}	5.890×10^{-3}	μ_x [–]	4.485×10^{-1}
$\Delta\mu_y$ [%]	2.141×10^{-3}	1.557×10^{-3}	1.557×10^{-3}	μ_y [–]	-7.344×10^{-1}
$\Delta\sigma_x^2$ [%]	6.949×10^{-2}	6.482×10^{-2}	6.482×10^{-2}	σ_x^2 [–]	5.004×10^{-5}
$\Delta\sigma_y^2$ [%]	3.332×10^{-2}	3.272×10^{-2}	3.272×10^{-2}	σ_y^2 [–]	1.045×10^{-5}
$\Delta\gamma_x$ [%]	1.000×10^{2}	2.573×10^{1}	2.573×10^{1}	γ_x [–]	-1.391×10^{-2}
$\Delta\gamma_y$ [%]	1.000×10^{2}	5.632×10^{0}	5.632×10^{0}	γ_y [–]	4.553×10^{-2}
Propagation time = 0.5 orbits					
$\Delta\mu_x$ [%]	1.453×10^{-1}	4.408×10^{-3}	4.408×10^{-3}	μ_x [–]	-6.866×10^{-1}
$\Delta\mu_y$ [%]	1.480×10^{-1}	1.329×10^{-2}	1.329×10^{-2}	μ_y [–]	-3.970×10^{-1}
$\Delta\sigma_x^2$ [%]	1.797×10^{-1}	1.291×10^{-1}	1.291×10^{-1}	σ_x^2 [–]	4.526×10^{-4}
$\Delta\sigma_y^2$ [%]	4.128×10^{-1}	1.148×10^{-1}	1.137×10^{-1}	σ_y^2 [–]	1.697×10^{-3}
$\Delta\gamma_x$ [%]	1.000×10^{2}	4.280×10^{-1}	4.273×10^{-1}	γ_x [–]	2.843×10^{-1}
$\Delta\gamma_y$ [%]	1.000×10^{2}	3.009×10^{0}	3.007×10^{0}	γ_y [–]	8.224×10^{-2}
Propagation time = 10 orbit					
$\Delta\mu_x$ [%]	5.724×10^{-1}	2.194×10^{-2}	2.194×10^{-2}	μ_x [–]	-6.834×10^{-1}
$\Delta\mu_y$ [%]	6.379×10^{-1}	7.325×10^{-2}	7.325×10^{-2}	μ_y [–]	-3.956×10^{-1}
$\Delta\sigma_x^2$ [%]	1.301×10^{0}	2.248×10^{-1}	1.805×10^{-1}	σ_x^2 [–]	1.858×10^{-3}
$\Delta\sigma_y^2$ [%]	6.783×10^{-1}	4.992×10^{-1}	4.828×10^{-1}	σ_y^2 [–]	6.742×10^{-3}
$\Delta\gamma_x$ [%]	1.000×10^{2}	3.165×10^{-1}	3.026×10^{-1}	γ_x [–]	5.517×10^{-1}
$\Delta\gamma_y$ [%]	1.000×10^{1}	3.165×10^{-1}	3.026×10^{-1}	γ_y [–]	1.694×10^{-1}
Propagation time = 30 orbit					
$\Delta\mu_x$ [%]	5.464×10^{0}	1.054×10^{-1}	1.054×10^{-1}	μ_x [–]	-6.507×10^{-1}
$\Delta\mu_y$ [%]	5.124×10^{0}	3.332×10^{-1}	3.332×10^{-1}	μ_y [–]	-3.806×10^{-1}
$\Delta\sigma_x^2$ [%]	7.363×10^{0}	1.893×10^{0}	1.346×10^{0}	σ_x^2 [–]	1.813×10^{-2}
$\Delta\sigma_y^2$ [%]	9.658×10^{0}	1.707×10^{0}	2.924×10^{-1}	σ_y^2 [–]	5.542×10^{-2}
$\Delta\gamma_x$ [%]	1.000×10^{2}	2.409×10^{0}	2.121×10^{0}	γ_x [–]	1.317×10^{0}
$\Delta\gamma_y$ [%]	1.000×10^{2}	4.838×10^{0}	6.294×10^{-1}	γ_y [–]	4.618×10^{-1}

Table 1: Mean, variance, and skewness relative error for the first two components x and y of the state vector calculated using DAHO-k (k = 1,2,3) with respect to DAMC-8 results in percentage for the 2-body dynamics test case.

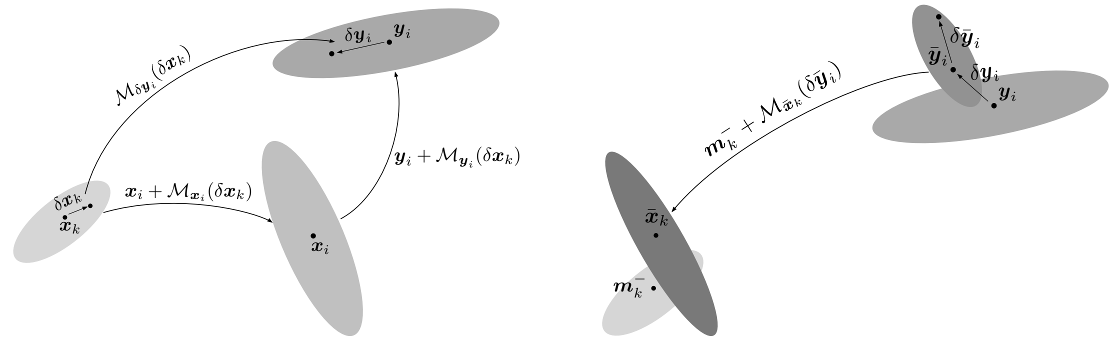

(a) Direct maps representation (b) Inverse map representation

Figure 5: Sketch of the Taylor maps involved in the construction of the DA-base map inversion nonlinear filter.

and the measurement function. Consider now the minimum number of independent measurements for which the previous map is invertible. The inverse map is a Taylor expansion of the state at t_k with respect to deviations $\delta \boldsymbol{y}_i$ of the measured variables, and defines the relation between the state variable and the observed data. At this point we can define the deviation of the predicted measurement with respect to the real measurement coming from the sensors as a DA variable, and use this variable to evaluate the inverse map. The result of this operation is another Taylor polynomial that instead of being centered on the predicted measurement is centered on the real one. The main cumulants of this map can be computed as described in the previous section, with the assumption that the statistics of the measurements is Gaussian. The computed mean and covariance are exploited to update the knowledge of $\boldsymbol{x}_k$ using a linear update scheme. This can be done for groups of measurements for which the dimension of measurement vector $\boldsymbol{y}_i$ is equal to the dimension of the state vector, and the map is invertible.

The resulting method can be summarized as follows. Define the current estimate at time of interest t_k as a DA variable; i.e., $[\boldsymbol{x}_k] = \boldsymbol{m}_k^- + \delta \boldsymbol{x}_k$. At time t_i when a measurement becomes available, propagate the current state forward/backward in time to obtain the state $\boldsymbol{x}_i$ at time t_i. The result assumes the form of the following high-order Taylor expansion map

$$[\boldsymbol{x}_i] = \boldsymbol{x}_i + \mathcal{M}_{\boldsymbol{x}_i}(\delta \boldsymbol{x}_k). \tag{28}$$

Then, use the measurement equation to compute the predicted measurement, obtaining

$$[\boldsymbol{y}_i] = \boldsymbol{h}(\boldsymbol{x}_i) = \boldsymbol{y}_i + \mathcal{M}_{\boldsymbol{y}_i}(\delta \boldsymbol{x}_k), \tag{29}$$

where $\boldsymbol{h}$ represents the measurement function. Next step consists in defining an origin preserving map

$$\delta \boldsymbol{y}_i = [\boldsymbol{y}_i] - \boldsymbol{y}_i = \mathcal{M}_{\delta \boldsymbol{y}_i}(\delta \boldsymbol{x}_k). \tag{30}$$

Figure 5(a) can be used by the reader to better understand the meaning of Maps (28)–(30).

This polynomial map can be inverted if two conditions are satisfied: the map must be square and all the measurements must be independent. If these requirements are satisfied, we can invert Map (30) using ad-hoc algorithms implemented in COSY-Infinity, obtaining

$$\delta \boldsymbol{x}_k = \mathcal{M}_{\delta \boldsymbol{x}_k}(\delta \boldsymbol{y}_i). \tag{31}$$

We now evaluate Map (31) in $[\Delta \boldsymbol{y}_i] = (\bar{\boldsymbol{y}}_i - \boldsymbol{y}_i) + \delta \bar{\boldsymbol{y}}_i$, where $\bar{\boldsymbol{y}}_i$ is the actual measurement coming from the sensors, and by adding to the result the initial estimate we obtain

$$[\bar{\boldsymbol{x}}_k] = \boldsymbol{m}_k^- + \mathcal{M}_{\bar{\boldsymbol{x}}_k}(\delta \bar{\boldsymbol{y}}_i). \tag{32}$$

Note that whereas Map (31) is centered on the predicted measurement, Map (32) is centered on the real observed data ($\delta \bar{\boldsymbol{y}}_i$ represents a deviation from it). This is a consequence of the evaluation of Map (31) in $[\Delta \boldsymbol{y}_i] = (\bar{\boldsymbol{y}}_i - \boldsymbol{y}_i) + \delta \bar{\boldsymbol{y}}_i$, which also causes $\mathcal{M}_{\bar{\boldsymbol{x}}_k}(\delta \bar{\boldsymbol{y}}_i)$ to be no more origin preserving. Hence, Taylor polynomial (32) represents the projection of the observed data on the state space at time t_k; i.e., if we evaluate this map in zero, we obtain the state vector $\bar{\boldsymbol{x}}_k$ that exactly produces measurements $\bar{\boldsymbol{y}}_i$, as shown in Figure 5(b). In the same figure the difference between $\delta \bar{\boldsymbol{y}}_i$ and $\delta \boldsymbol{y}_i$ is underlined.

We can now apply Eq. (23) to Taylor expansion (32) to compute the statistics of random variable $\bar{\boldsymbol{x}}_k$ and, in particular, the first two moments $\bar{\boldsymbol{m}}_k$ and $\bar{\boldsymbol{P}}_k$. The computed mean can be treated as a "measure"of the state at time t_k, with measurement error defined by $\bar{\boldsymbol{P}}_k$ and therefore can be used to update the initial estimate and error covariance, using the least square method. This can be done using the Kalman filter update equations that, applied to the current problem, reads

$$\boldsymbol{K} = \boldsymbol{P}_k^- \left(\boldsymbol{P}_k^- + \bar{\boldsymbol{P}}_k \right)^{-1}, \tag{33}$$

$$\boldsymbol{m}_k^+ = \boldsymbol{m}_k^- + \boldsymbol{K} \left(\bar{\boldsymbol{m}}_k - \boldsymbol{m}_k^- \right), \tag{34}$$

$$\boldsymbol{P}_k^+ = (\boldsymbol{I} - \boldsymbol{K}) \boldsymbol{P}_k^- (\boldsymbol{I} - \boldsymbol{K})^T + \boldsymbol{K} \bar{\boldsymbol{P}}_k \boldsymbol{K}^T, \tag{35}$$

where $\boldsymbol{P}_k^-$ is the initial error covariance matrix, $\boldsymbol{m}_k^+$ the updated mean at time t_k and $\boldsymbol{P}_k^+$ the related updated covariance matrix. When another measurement becomes available, we can define the state at time t_k as a new DA variable, centered in the new computed mean $\boldsymbol{m}_k^+$, and iterate the process.

We said that Map (30) must be square in order to be invertible. It follows that if the measurement vector has smaller dimension than the state vector, after the first measurement set is received we can not proceed with the filtering procedure, but we have to wait for additional measurements. When the number of scalar measurements equals the dimension of the state variable, we can define an augmented measurement vector that can be used to build Maps (29) and (30).

Once the final estimate of the state at time t_k is obtained, the statistics of the solution can be computed at any time by using the DAHO-k method proposed in the previous section.

SIMULATION RESULTS

In this section, we present simulations for a spacecraft orbiting around the Earth in a two-body dynamical framework. The governing equation of motions and the initial conditions for the considered orbit are presented in Eqs. (26) and (27). Initially, the spacecraft state is assumed to be deviated from the real state, with position uncertainties of 100 km and velocity uncertainties of 7×10^{-4} km/s. For the measurement model, we assume to measure the range and the lines-of-sight from the vehicle to the Earth. The measurement noise is assumed to be 0.1 m for range measurement and 0.1 arcsec for angle measurement. A set of pseudo-measurements are computed based on the reference trajectory with a 22-minutes increment (6 measures in each orbital period) and a horizon of five orbital periods is analyzed. In this case, the considered reference time t_k is the initial time (i.e., t_0).

First of all, Figure 6 shows how the update step of the filtering algorithm (presented in Eqs. (34) and (35)) works. The initial statistics, here represented using only the first two moments, $(\boldsymbol{m}_0^-, \boldsymbol{P}_0^-)$

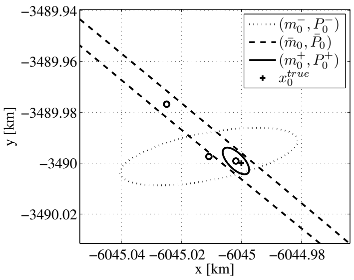

Figure 6: Estimated mean and error covariance projection on the x-y plane.

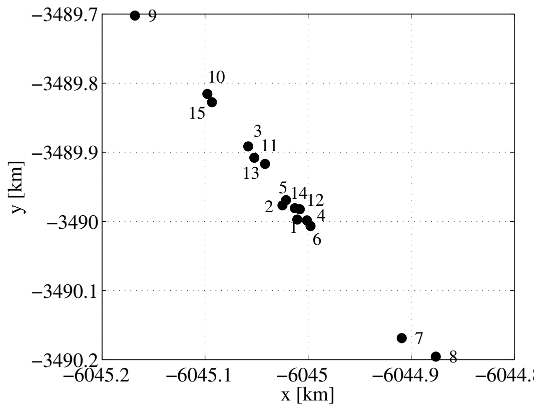

Figure 7: Measurements projection on the x-y state space. Measurements are labeled with the iteration number.

is corrected using the measurement projection on the state space $(\bar{\boldsymbol{m}}_0, \bar{\boldsymbol{P}}_0)$ to obtain a more accurate estimate of the solution $(\boldsymbol{m}_0^+, \boldsymbol{P}_0^+)$. Notice that since we are not making any assumption on the state variable statistics, the error covariance does not necessarily represent the confidence region. However, since in the considered case the state pdf is close to a Gaussian pdf, the confidence region is close to the ellipsoid associated to the covariance matrix. We can also notice that the real state is included in the updated ellipsoid.

In Figure 7 the projection on the state space of the observed data are plotted, whereas Figure 8 shows the estimated mean and covariance ellipsoid projection on the x-y plane for every filtering time step. Comparing these two figures, we can see that the estimation uncertainty is related and correctly matches the measurement noise.

Figure 9 shows the magnitude of the absolute position and velocity errors, that is, the magnitude of the difference between the updated mean and the true state. In Figure 10 a comparison of the relative position and velocity errors between the proposed DA-based map inversion filter, the EKF, and UKF is plotted. The results underline that the EKF does not perform well as compared to the other filters. Since the DA-MIF is a higher-order filter and the UKF can represent the estimate statistics with a second order accuracy, this clearly explains the importance of nonlinear orbit uncertainty propagation. In this case, the UKF performs as the proposed high-order filter. However, it has been demonstrated that if we increase the initial uncertainty, the measurement noise, and/or the filtering time step, the performance of the UKF drops off. At this purpose, Figure 11 reports the results of a simulation where bigger measurement noises are considered; i.e., 0.1 km for range measurement

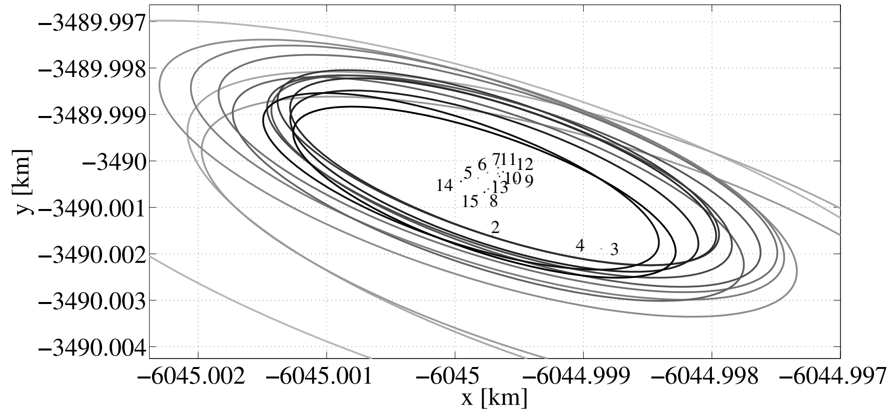

Figure 8: Convergence process of the computed mean and covariance ellipsoid projection on the x-y plane. The estimated state is labeled with the iteration number and data are plotted in grey scale (newer data are darker).

and 1 arcsec for angle measurement. From this figure, it is possible to see that while the UKF diverges, the DA-based map inversion filter still guarantees convergence (even if, of course, with worse accuracy with respect to the previous test case).

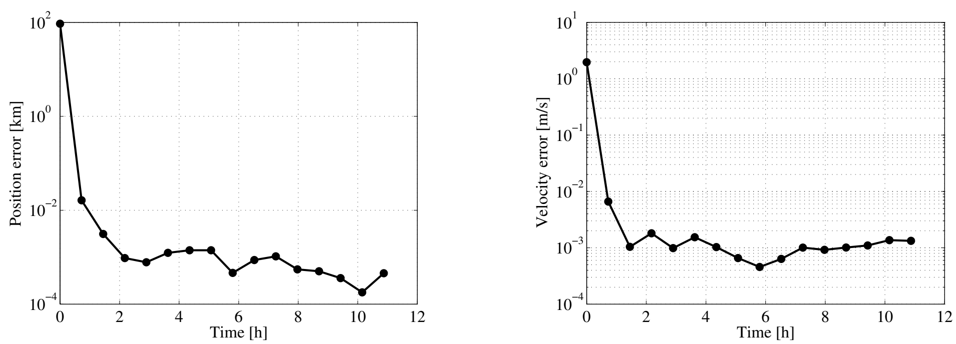

(a) Position absolute error

(b) Velocity absolute error

Figure 9: Filter accuracy with a 22-minutes increment measurement update.

CONCLUSIONS

In this paper the problem of nonlinear filtering has been addressed. Working in the differential algebra framework we derived a high-order filter, called differential algebra-based map inversion filter. This filtering algorithms is based on nonlinear mapping of statistics and linear update scheme, in which only the pdf of the measurements is constrained to be Gaussian. No hypothesis on the state probability density function is made. The proposed filter was compared with the conventional extended Kalman filter and the unscented Kalman filter based on a Earth-orbiting spacecraft in a two-body problem frame. The filter simulations were carried out assuming the dynamics of the system are perfectly known, but there are errors in the initial state and in the measurements. The results showed that the proposed filter provides better performance that the linearized solution and,

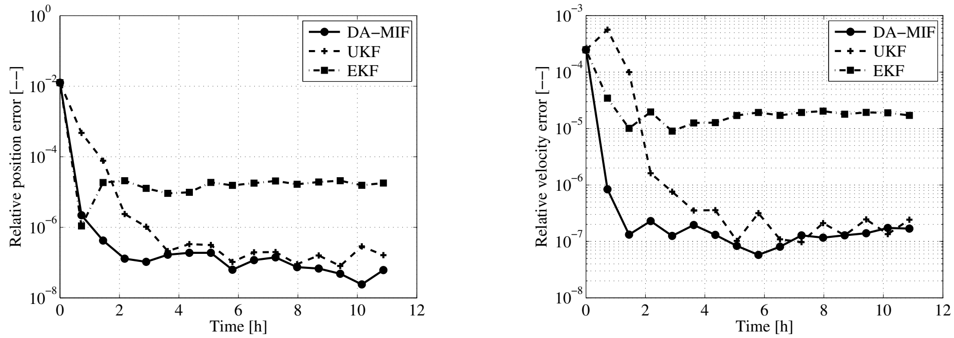

(a) Position relative error (b) Velocity relative error

Figure 10: Filters accuracy comparison with a 22-minutes increment measurement update.

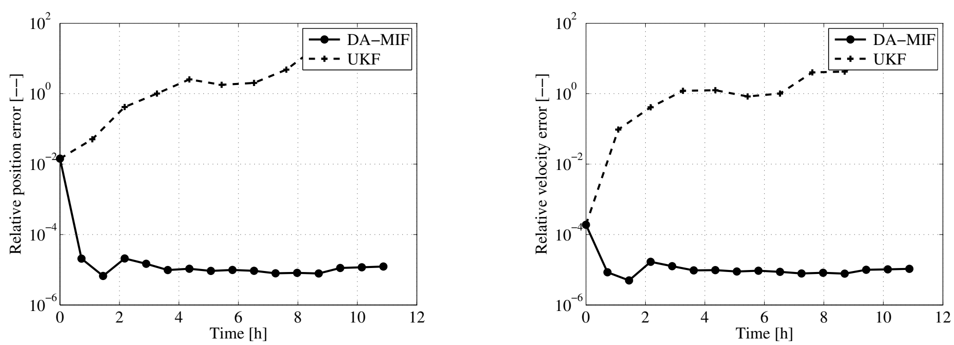

(a) Position relative error (b) Velocity relative error

Figure 11: Filters accuracy comparison with measurement noises of 0.1 km for range measurement and 1 arcsec for angle measurement.

in some cases (i.e., when the initial uncertainty, the measurement noise, and/or the filtering time step are large), also than the unscented Kalman filter.

REFERENCES

[1] G. Bierman, *Factorization methods for discrete sequential estimation*. Dover Publications, 2006.

[2] O. Montebruck and E. Gill, "Satellite Orbits," 2000.

[3] S. Julier and J. Uhlmann, "Unscented filtering and nonlinear estimation," *Proceedings of the IEEE*, Vol. 92, No. 3, 2004, pp. 401–422.

[4] S. Julier, J. Uhlmann, and H. Durrant-Whyte, "A new approach for filtering nonlinear systems," *American Control Conference, 1995. Proceedings of the*, Vol. 3, IEEE, 1995, pp. 1628–1632.

[5] R. Park and D. Scheeres, "Nonlinear mapping of Gaussian statistics: theory and applications to spacecraft trajectory design," *Journal of guidance, Control, and Dynamics*, Vol. 29, No. 6, 2006, pp. 1367–1375.

[6] R. Park and D. Scheeres, "Nonlinear semi-analytic methods for trajectory estimation," *Journal of guidance, control, and dynamics*, Vol. 30, No. 6, 2007, pp. 1668–1676.

[7] M. Majji, J. Junkins, and J. Turner, "A High Order Method for Estimation of Dynamic Systems," *The Journal of the Astronautical Sciences*, Vol. 56, No. 3, 2008, pp. 1–32.

[8] V. Vittaldev, R. Russell, N. Arora, and D. Gaylor, "Second-order Kalman filters using multi-complex step derivatives," *AAS/AIAA Space Flight Mechanics Meeting, Charleston, SC*, No. AAS 12-204, 2012.

[9] M. Valli, R. Armellin, P. Di Lizia, and M. Lavagna, "Nonlinear management of uncertainties in celestial mechanics," *AAS/AIAA Space Flight Mechanics Meeting, Charleston, SC*, No. AAS 12-264, 2012.

[10] M. Berz, *Differential Algebraic Techniques, Entry in Handbook of Accelerator Physics and Engineering*. New York: World Scientific, 1999.

[11] M. Berz, K. Makino, and K. Shamseddine, *Modern map methods in particle beam physics*, Vol. 108. Academic Press, 1999.

[12] M. Valli, R. Armellin, P. Di Lizia, and M. Lavagna, "Nonlinear Filtering Methods for Spacecraft Navigation Based on Differential Algebra," *1st IAA Conference on Dynamics and Control of Space Systems, Porto, Portugal*, 2012.

[13] M. Berz, *Modern Map Methods in Particle Beam Physics*. Academic Press, 1999.

[14] M. Berz, *The new method of TPSA algebra for the description of beam dynamics to high orders*. Los Alamos National Laboratory, 1986. Technical Report AT-6:ATN-86-16.

[15] M. Berz, "The method of power series tracking for the mathematical description of beam dynamics," *Nuclear Instruments and Methods A258*, 1987.

[16] M. Berz, *Differential Algebraic Techniques, Entry in Handbook of Accelerator Physics and Engineering*. New York: World Scientific, 1999.

[17] M. Berz and K. Makino, *COSY INFINITY version 9 reference manual*. Michigan State University, East Lansing, MI 48824, 2006. MSU Report MSUHEP060803.

[18] R. Park and D. Scheeres, "Nonlinear Mapping of Gaussian Statistics: theory and Applications to Spacecraft trajectory Design," *Journal of Guidance, Control and Dynamics*, Vol. 29, No. 6, 2006.

[19] G. Casella and R. Berger, *Statistical inference*. Duxbury Press, 2001.

[20] L. Isserlis, "On a formula for the product-moment coefficient of any order of a normal frequency distribution in any number of variables," *Biometrika*, Vol. 12, No. 1 and 2, 1918.

[21] R. Kan, "From moments of sum to moments of product," *Journal of Multivariate Analysis*, Vol. 99, No. 3, 2008.

[22] D. Griffith, J. Turner, and J. Junkins, "An embedded function tool for modeling and simulating estimation problems in aerospace engineering," *Advances in the Astronautical Sciences*, Vol. 119, No. AAS 04-148, 2004.